

DeepTree: Accurate Airway Tree Segmentation in CT Scans via Anatomy-aware Multi-class Segmentation and Deep Breakage Connection

Paper Submission # 868

No Institute Given

Abstract. Intrathoracic airway segmentation from computed tomography (CT) is a frequent prerequisite for various respiratory disease analysis such as chronic obstructive pulmonary disease (COPD), asthma and lung cancer. Due to the low contrast and imaging noise execrated at peripheral branches, and the topological-complexity and intra-class imbalance of the entire airway tree, it is still challenging for the deep learning-based approaches to segment deeper airway branches and avoiding the segmentation breakage within branches. To address this, we propose a two-stage airway segmentation method. At 1st-stage, motivated by the natural airway anatomy, we formulate a simple yet effective anatomy-aware multi-class segmentation problem to intuitively handle the intra-class imbalance and the large context variation of different branches. At 2nd-stage, we introduce a new breakage attention map (calculated by morphological operations), which can highlight the segmentation breakage within disconnected branches. We also develop a domain-specific simulation method to generate sufficient training samples that cover various branch breaking conditions. Then, a 2nd-stage breakage connection network is trained using the early fusion of locally cropped CT and breakage attention map, where outputs are merged with the initial segmentation to generate a complete airway tree. Extensive experiments are conducted using an airway segmentation dataset containing 90 cases. We demonstrate that our proposed method achieves significantly improved performance over the previous state-of-the-art methods by extracting at least 8.2% more detected tree length and 4.3% more tree branches.

1 Introduction

Respiratory diseases impose an immense health burden worldwide as millions of people die each year because of chronic obstructive pulmonary disease (COPD), asthma, lung cancer, and etc [7]. As one of the major organs in the respiratory system, intrathoracic airway has been studied broadly for disease screening and diagnosis, surgical navigation, and treatment effects evaluation [6, 16]. Computed tomography (CT)-based quantitative lung analysis provides valuable information, where airway tree segmentation is often a prerequisite for various downstream tasks. Because of the complexity of tree topology in 3D and hundreds of slices to be annotated, manual airway segmentation is an extremely tedious process costing up to 7 hours for one case [18].

Automatic airway segmentation in CT has been extensively explored for decades. Early works involves thresholding, morphology, graph or conventional learning-based methods [8, 17, 19, 21], where the extracted airway tree lengths are mostly below 65% [9]. Recent deep learning-based methods achieves significantly improved performance [1, 2, 5, 11–13, 22–24], especially for those equipped with 3D deep networks exploring the 3D continuity of tree branches. Jin et al. first train a 3D fully convolutional network (FCN) followed by a fuzzy connectivity-based segmentation refinement [5]. Selvan et al. explored the graph neural network to incorporate features of neighborhood [13]. Another main line of research lies in designing new loss functions to enhance airway’s tubular connectivity or leverage the inter- and intra-class imbalance problem. For example, a radial distance loss is presented to increase airway’s topology in [20], and a distance-weighted Tversky loss (named general union loss) is introduced to resolve the intra-class imbalance in [24]. Zheng et al. recently proposes to alleviate the airway gradient erosion and dilation problem based on the quantification of local class imbalance in the loss function [23].

Despite the boosted performance of deep learning-based approaches, there are still challenges leading to unsatisfactory results. (1) By nature, airway possesses a tree topology with locally elongated branches, which have large scale and context differences at various anatomic levels. For example, diameters of trachea and small bronchus are differed by 10 to 20 times, while locations and surrounding tissues are also completely different (mediastinum vs lung parenchyma). Substantial intra-class imbalance and context differences increase the learning difficulty especially for those thin branches at peripheral locations. Although various strategies are developed recently [20, 23, 24], missing branches are still commonly observed (Fig. 1 (a)). (2) Because of the high uncertainty in distal bronchi who yield poor contrast between airway lumen and wall, the presence of segmentation breakage is almost unavoidable (Fig. 1 (c)). Connecting the breakage is another unsolved problem. Recent work [14] has investigated new topology-preserving loss (clDice) to enforce the segmentation connectivity, however, it requires a significantly longer training time and has a markedly inferior performance as compared to other state-of-the-art methods [12, 23, 24].

In this work, we propose a two-stage airway segmentation framework, named DeepTree, to tackle these challenges. At 1st-stage, motivated by the natural airway anatomy, we formulate a simple yet effective anatomy-aware multi-class segmentation problem to intuitively handle the intra-class imbalance and the large context variation of branches at different levels. Specifically, we decompose the entire airway tree into 3 classes and directly learn the class-specific features, i.e., trachea and left/right main bronchi (large branches mostly at mediastinum), bronchi up to segmental level, and the rest of bronchi visible in CT (small branches deep into lung parenchyma). Beside the multi-class formulation, we also incorporate the general union loss [24], which is applied to the whole airway tree to further leverage the severe intra-class imbalance problem. At 2nd-stage, we aim to connect the breaking branches commonly existed in the initial segmentation. To achieve that, we introduce a new breakage atten-

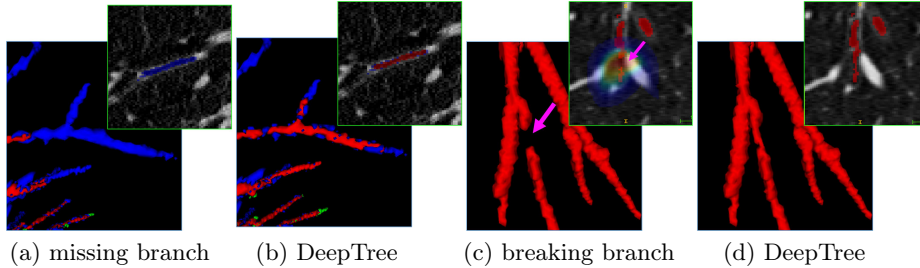


Fig. 1: Examples of airway tree segmentation with missing branches (a) and segmentation breakage (c) produced using the leading method [23]. The corresponding segmentation of proposed DeepTree are shown in (b) and (d). Missing branches are colored in blue and the breakage is indicated by the pink arrow. Note that the breakage attention map is overlaid with CT slice of breaking branch in (c).

tion map to highlight the breaking area in disconnected branches (see Fig. 1 for an illustration). We also develop a domain-specific simulation method to generate sufficient training samples that contains various branch breaking conditions. Then, a 2nd-stage breakage connection deep network is trained using the early fusion of CT and the breakage attention map cropped around the local breaking region. Finally, outputs of 2nd-stage are merged with the initial segmentation to generate a complete airway segmentation. Extensive experiments are carried out using an airway segmentation dataset containing 90 cases. We demonstrate that DeepTree achieves significant improvements of at least 8.2% and 4.3% more detected tree length and tree branches, respectively, as compared to previous leading approaches such as [14, 23, 24].

2 Method

Fig. 2 depicts an overview of our proposed airway segmentation method, DeepTree, which consists of three major components: (1) anatomy-aware multi-class airway segmentation; (2) breakage attention calculation and domain-specific breakage training data simulation; and (3) 2nd-stage deep breakage connection.

2.1 Anatomy-aware Multi-class Segmentation

As discussed, airway tree structure poses the unique challenge for segmentation, especially due to the intra-class imbalance between different levels of branches. As analyzed in [24], there exists the gradient erosion phenomenon during the network training due to the intra-class imbalance, which makes the network ineffective to learn features of small airway branches. To alleviate this, we propose a simple yet effective strategy by formulating the task to a multi-class segmentation problem, where each class has its distinguished airway branch size range and class-specific features can be naturally learned. This also helps to explicitly differentiate the anatomic context of different branches, e.g., trachea in

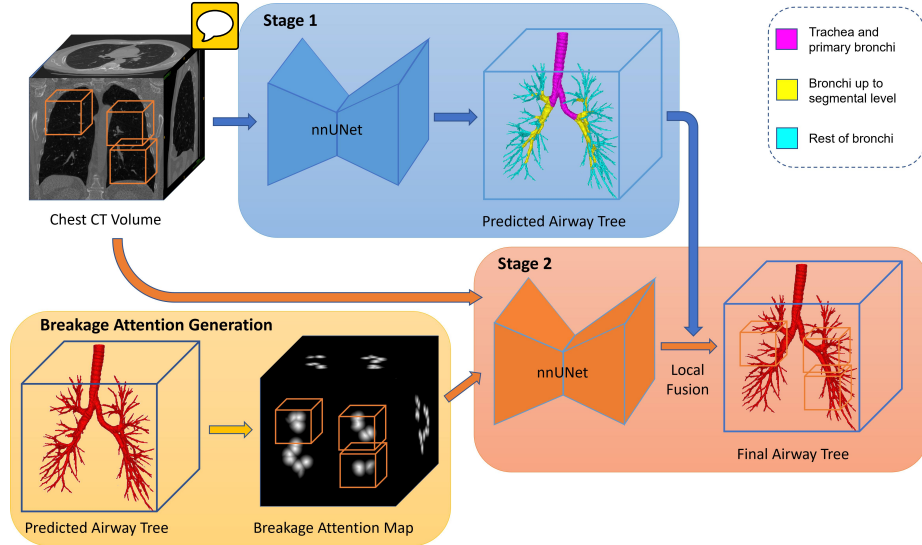


Fig. 2: Overall workflow of our proposed breakage reducing airway segmentation framework named DeepTree. Note that for the inference and training of 2nd-stage, only patches around the breakage attention are used as inputs to the network.

mediastinum and small bronchus in parenchyma. Based on the airway anatomy, we decompose the entire airway tree Y into three classes: (1) trachea+left/right main bronchi Y^L , bronchi up to segmental level Y^M , and the rest of bronchi Y^S . Y^L can be easily derived. For the rest of two classes, we set an airway branch to Y^S if its average lumen diameter is ≤ 2 mm in our experiment for simplicity. Let $\hat{Y} = [\hat{Y}^L, \hat{Y}^M, \hat{Y}^S]$ be the prediction of three classes. We formulate the anatomy-aware multi-class (AMC) airway segmentation as follows:

$$\mathcal{L}_M(\hat{Y}, Y) = \mathcal{L}_S(\hat{Y}^L, Y^L) + \mathcal{L}_S(\hat{Y}^M, Y^M) + \mathcal{L}_S(\hat{Y}^S, Y^S), \quad (1)$$

where \mathcal{L}_S can be any commonly used segmentation loss, e.g., Dice loss and/or cross-entropy (CE) loss. Considering that the general union loss (GUL), which is a distance-weighted Tversky loss [15], has been shown to be effective in airway segmentation [24], we further applied it to the entire airway label and combined it with our AMC segmentation.

2.2 Breakage Attention Generation

Another major problem of airway segmentation is the presence of **breakage** in the predicted airway mask. To connect the breaking branch, we first introduce a novel breakage attention map to highlight the breaking area. Given an initial airway segmentation result \hat{Y} , we apply the connected component analysis to label each component \hat{Y}_k leading to a main connected airway tree with the rest disconnected segments. Let C_k denote the number of connected components.

Then, for each component \hat{Y}_k , a 3D Euclidean distance transformation map D_k is calculated [10] to provide the shortest distance between a background voxel j and component \hat{Y}_k . Next, let C_{min} denote the component which has the shortest distance to voxel j among all components $\hat{Y}_k, k \in \{1, 2, \dots, C_k\}$. Then, the raw breakage attention value H at a location j is determined as the second shortest distance among all components:

$$H(j) = \min_{k \in \{1, 2, \dots, C_k\}, k \neq C_{min}} D_k(j) \quad (2)$$

The raw breakage attention map H can highlight the breaking regions of disconnected branches. To be utilized in the 2nd-stage training, H is further normalized by a Sigmoid function $\bar{H} = \text{Sigmoid}(\alpha - H)$, where α is the parameter for controlling breakage attention range and we set it to 5 in our experiment. From Fig. 1, we can see that \bar{H} at a breakage location normally forms a 3D ball-like intensity distribution.

2.3 Deep Breakage Connection & Simulated Training Data

For training the 2nd-stage breakage connection deep network, we need sufficient training samples that contain various breaking conditions at different airway branch locations. However, there is no breakage in the ground truth (GT) labels. Therefore, we sort to simulate the branch breaking conditions using GT labels for the 2nd-stage training. To achieve this, a domain-specific breakage simulation method is developed as follow: (1) For a GT airway mask in the training set, we first extract its curve skeleton using a robust minimum-cost path approach that avoids generating the false centerlines [4]. (2) A random subset 50% of peripheral branches are selected. For a chosen branch, we randomly select a continuous subset of 10%-30% skeleton voxels and set them to a different value (as breakage label). (3) A skeleton-to-volume propagation algorithm [4] is applied to the breakage-simulated skeleton to generate the final volumetric breakage GT labels, which are denoted as Y^B . In this way, various breakage conditions can be simulated using the training GT labels.

With sufficient training samples, we train a breakage connection network to connect the breaking branches. Since breakage happens locally, we use small local patches for the 2nd-stage training. First, the center of each breakage highlighted in the breakage attention map is determined. Next, a local CT and breakage attention patch (X' and \bar{H}') with the size of $64 \times 64 \times 64$ is cropped applying a random 3D spatial shifting. Then, a 3D breakage connection network is trained using the early fusion of X' and \bar{H}' to predict the breakage \hat{Y}^B :

$$\hat{Y}^B = \mathcal{F}(X', \bar{H}'; \mathbf{W}) \quad (3)$$

$$\mathcal{L}_{\mathbb{B}} = \mathcal{L}_{\mathbb{S}}(\hat{Y}^B, Y^B), \quad (4)$$

where $\mathcal{F}(\cdot)$ and \mathbf{W} denote the 2nd-stage breakage connection network function and network parameters, respectively. Y^B and \hat{Y}^B indicate the GT and predicted

Table 1: Quantitative comparison with previous state-of-the-art methods.

Methods	BD (%)	TLD (%)	Precision (%)
Juarez et al. [2]	69.2±25.4	53.5±20.9	99.9±0.1
UNet++ [25]	87.2±10.9	74.2±11.8	99.3±0.6
clDice [14]	88.0±10.2	76.2±11.1	99.1±0.7
nnUNet [3]	89.1±5.5	76.1±6.4	99.9 ± 0.1
WingsNet [24]	89.2±5.8	77.1±5.7	99.0±0.8
Qin et al. [12]	90.9±8.8	80.7±9.9	98.4±1.0
Zheng et al. [23]	91.1±5.5	80.1±6.6	98.9±0.7
DeepTree	95.4 ± 3.6	88.9 ± 4.5	97.2±1.1

breakage, respectively. When performing the inference, the outputs \hat{Y}^B at all breaking locations are combined with the initial segmentation and the largest connected component is extracted as the final airway segmentation.

3 Experimental Results

Dataset. For evaluation, we conduct our experiment on 90 chest CT scans collected in the Binary Airway Segmentation Dataset [11] and use the same data split in [24] with 50, 20 and 20 cases for training, validation and testing, respectively. Note that for the 20 testing cases, three experts are asked to further curate the GT labels originally provided in the dataset [11], since true airway branches were observed to miss in the original GT. We evaluate the performance of all methods using the curated/improved GT labels in testing cases, however, no additional manual curation is conducted on the training cases.

Implementation details. We adopt the nnUNet [3] as our backbone for both stages because of its high accuracy on many medical image segmentation tasks. We adapt and modify the original nnUNet architecture to better accommodate to the airway task. Specifically, we reduce the downsampling operation to 3 times (originally 5 times) with four levels of spatial resolutions considering the very small branches at peripheral sites. Meanwhile, we enlarge the width of the convolutional layers at the deeper blocks to increase the learning capacity. For the loss function, we implement and use the combination of multi-class Dice + CE loss and GUL for the 1st-stage, while adopt the default Dice + CE loss for the 2nd-stage. The total training epochs for both stages is 500. The rest settings are the same as the default nnUNet setup.

Evaluation metrics. We adopt three most important airway evaluation metrics as commonly adopted in [12, 23, 24]: branches detected (BD), tree length detected (TLD) and precision. Similarly, we also exclude the trachea and left/right main bronchi for evaluation of all three metrics.

Quantitative Results and Comparisons to Previous State-of-the-art Methods. Our quantitative results and comparisons to state-of-the-art methods are tabulated in Table 1. It is observed that methods without tailoring to the airway segmentation normally have inferior performance. For example, the de-

Table 2: Quantitative ablation results for the airway tree segmentation. GUL and AMC represent the general union loss [24] and the proposed anatomy-aware multi-class segmentation, respectively. nnUNet* is the adapted version for airway tree segmentation.

Backbone	1st-stage		2nd-stage	Metrics		
	AMC	GUL		BD (%)	TLD (%)	Precision (%)
nnUNet*	—	—	—	90.3±5.1	78.1±6.7	99.8 ± 0.2
	✓	—	—	91.9±4.7	81.0±5.9	99.4±0.4
	—	✓	—	93.3±4.4	83.1±5.9	98.8±0.6
	✓	✓	—	95.1±3.6	88.2±4.7	97.4±1.1
nnUNet*	—	—	✓	91.2±5.2	79.6±6.5	99.7±0.3
	✓	—	✓	92.5±4.5	82.3±5.7	99.4±0.4
	—	✓	✓	94.1±4.0	85.9±5.8	98.4±0.7
	✓	✓	✓	95.4 ± 3.6	88.9 ± 4.5	97.2±1.1

tected branch and tree length of UNet++ [25], cIDice [14] and default nnUNet [3] are generally less than those of [12, 23, 24] that are specifically designed for airway segmentation. Among the airway segmentation state-of-the-art methods, two of them produce the previously best performance (91.1% BD and 80.7% TLD) by using the feature recalibration and attention distillation [12] or the local-imbalance & back-propagation based weighting schemes [23]. In comparison, our proposed DeepTree achieves significantly improved performance with 95.4% BD and 88.9% TLD, which have at least 4.3% more branches detected and 8.2% more tree length extracted. It also has the lowest standard derivation. For the slightly decreased precision, it is observed that some of the false positive segmentation of DeepTree is actually true airway branches that are still missed even in the curated GT labels. When evaluated using original GT labels provided by [11], DeepTree achieves 99.0% BD and 97.7% TLD, which are 1.8% and 4.4% higher than those by the method of [23]. While the precision of DeepTree on orginal GT labels is 86.9%, it drastically increase to 97.2% on curated GT labels.

Ablation Results. We conduct the ablation study to demonstrate the effectiveness of each component in the proposed DeepTree and results are shown in Table 2. Several conclusions can be drawn. First, the proposed anatomy-aware multi-class (AMC) method is effective to segment the airway tree. When applied to our adapted nnUNet* (second vs first row), AMC improves the performance by extracting ~3% and ~2% more tree length and branches, respectively, while maintaining the almost same high precision. This validates our assumption that decomposing the whole airway tree into 3 classes based on their anatomic levels is beneficial to handle the intra-class imbalance and the large context variation of airway tree. Second, AMC and GUL are complementary to each other. Although the AMC or GUL alone can help better segment the airway, their combination further significantly improves the results (forth vs second and third rows). For instance, even if GUL is already utilized in the nnUNet* model to balance the

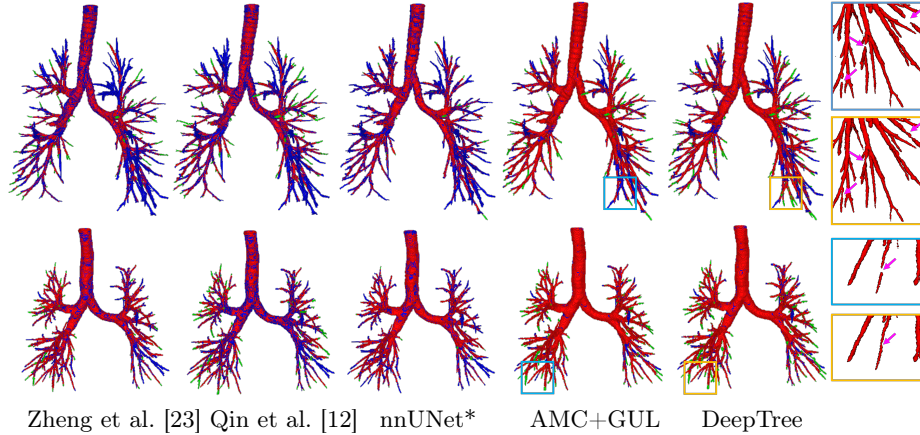


Fig. 3: Results of airway tree segmentation using different methods. Red, blue and green colors represent the true positive, false negative and false positive segmentation, respectively. For our proposed DeepTree, we further demonstrate the effectiveness of the 2nd-stage by zooming the breakages (indicated by pink arrows) in the output of 1st-stage (AMC+GUL).

intra-class weights, combining it with the AMC still leads to an additionally $\sim 5\%$ and $\sim 2\%$ increasing in the extracted tree length and tree branches. Finally, the introduced breakage connection method in 2nd-stage consistently improves all the initial segmentation from the 1st-stage (row 5-8 vs row 1-4) while maintaining similar precision. For example, the detected tree length has been improved by 1.6% when averaged among four different 1st-stage results with the maximum improvement of 2.8% (row 7 vs row 3). This indicates that the proposed breakage connection method may be universally applied to the elongated anatomic structure segmentation tasks, where segmentation breakage commonly exists. Qualitative results are shown in Fig. 3 to visually understand our improvement.

4 Conclusion

In this paper, we propose a new two-stage airway segmentation workflow. At 1st-stage, motivated by the natural airway anatomy, we formulate a simple yet effective anatomy-aware multi-class segmentation problem to intuitively handle the intra-class imbalance and the large context variation of airway branches. At 2nd-stage, we introduce a novel breakage attention map, which can highlight the breaking region within the disconnected branches. Using the early fusion of locally cropped CT and breakage attention map, a 2nd-stage breakage connection network is trained. The output of 1st- and 2nd-stage are merged to generate a complete airway tree. Extensive quantitative experiments demonstrate that our proposed DeepTree framework achieves significantly improved performance over the previous state-of-the-art methods [12, 14, 23, 24], by increasing at least 8.2% more detected tree length and 4.3% more detected branch.

References

1. Charbonnier, J.P., van Rikxoort, E.M., Setio, A.A., Schaefer-Prokop, C.M., van Ginneken, B., Ciompi, F.: Improving airway segmentation in computed tomography using leak detection with convolutional networks. *Medical Image Analysis* **36**, 52 – 60 (2017)
2. Garcia-Uceda Juarez, A., Selvan, R., Saghir, Z., Bruijne, M.d.: A joint 3d unet-graph neural network-based method for airway segmentation from chest cts. In: International workshop on machine learning in medical imaging. pp. 583–591. Springer (2019)
3. Isensee, F., Jaeger, P.F., Kohl, S.A., Petersen, J., Maier-Hein, K.H.: nnu-net: a self-configuring method for deep learning-based biomedical image segmentation. *Nature methods* **18**(2), 203–211 (2021)
4. Jin, D., Iyer, K.S., Chen, C., Hoffman, E.A., Saha, P.K.: A robust and efficient curve skeletonization algorithm for tree-like objects using minimum cost paths. *Pattern Recognition Letters* **76**, 32 – 40 (2016), special Issue on Skeletonization and its Application
5. Jin, D., Xu, Z., Harrison, A.P., George, K., Mollura, D.J.: 3d convolutional neural networks with graph refinement for airway segmentation using incomplete data labels. In: International workshop on machine learning in medical imaging. pp. 141–149. Springer (2017)
6. Kuwano, K., Bosken, C.H., Paré, P.D., Bai, T.R., Wiggs, B.R., Hogg, J.C.: Small airways dimensions in asthma and in chronic obstructive pulmonary disease. *American Review of Respiratory Disease* **148**(5), 1220–1225 (1993)
7. Levine, S.M., Marciniuk, D.D.: Global impact of respiratory disease: What can we do, together, to make a difference? *Chest* (2022)
8. Lo, P., Sporring, J., Ashraf, H., Pedersen, J.J., de Bruijne, M.: Vessel-guided airway tree segmentation: A voxel classification approach. *Medical Image Analysis* **14**(4), 527 – 538 (2010)
9. Lo, P., Van Ginneken, B., Reinhardt, J.M., Yavarna, T., De Jong, P.A., Irving, B., Fetita, C., Ortner, M., Pinho, R., Sijbers, J., et al.: Extraction of airways from ct (exact'09). *IEEE Transactions on Medical Imaging* **31**(11), 2093–2107 (2012)
10. Maurer, C.R., Qi, R., Raghavan, V.: A linear time algorithm for computing exact euclidean distance transforms of binary images in arbitrary dimensions. *IEEE Transactions on Pattern Analysis and Machine Intelligence* **25**(2), 265–270 (2003)
11. Qin, Y., Chen, M., Zheng, H., Gu, Y., Shen, M., Yang, J., Huang, X., Zhu, Y.M., Yang, G.Z.: Airwaynet: a voxel-connectivity aware approach for accurate airway segmentation using convolutional neural networks. In: International Conference on Medical Image Computing and Computer-Assisted Intervention. pp. 212–220. Springer (2019)
12. Qin, Y., Zheng, H., Gu, Y., Huang, X., Yang, J., Wang, L., Zhu, Y.M.: Learning bronchiale-sensitive airway segmentation cnns by feature recalibration and attention distillation. In: International Conference on Medical Image Computing and Computer-Assisted Intervention. pp. 221–231. Springer (2020)
13. Selvan, R., Kipf, T., Welling, M., Juarez, A.G.U., Pedersen, J.H., Petersen, J., de Bruijne, M.: Graph refinement based airway extraction using mean-field networks and graph neural networks. *Medical Image Analysis* **64**, 101751 (2020)
14. Shit, S., Paetzold, J.C., Sekuboyina, A., Ezhov, I., Unger, A., Zhylka, A., Pluim, J.P., Bauer, U., Menze, B.H.: eldice-a novel topology-preserving loss function for tubular structure segmentation. In: Proceedings of the IEEE/CVF Conference on Computer Vision and Pattern Recognition. pp. 16560–16569 (2021)

15. Slaehi, S.S.M., Erdogmus, D., Gholipour, A.: Tversky loss function for image segmentation using 3d fully convolutional deep networks. In: International workshop on machine learning in medical imaging. pp. 379–387. Springer (2017)
16. Smith, B.M., Traboulsi, H., Austin, J.H., Manichaikul, A., Hoffman, E.A., Bleecker, E.R., Cardoso, W.V., Cooper, C., Couper, D.J., Dashnaw, S.M., et al.: Human airway branch variation and chronic obstructive pulmonary disease. Proceedings of the National Academy of Sciences **115**(5), E974–E981 (2018)
17. Tschirren, J., Hoffman, E.A., McLennan, G., Sonka, M.: Intrathoracic airway trees: segmentation and airway morphology analysis from low-dose ct scans. IEEE Transactions on Medical Imaging **24**(12), 1529–1539 (Dec 2005)
18. Tschirren, J., Yavarna, T., Reinhardt, J.M.: Airway Segmentation Framework for Clinical Environments. In: Second International Workshop on Pulmonary Image Analysis. pp. 227–238. London, UK (2009)
19. Van Rikxoort, E.M., Baggerman, W., Van Ginneken, B.: Automatic segmentation of the airway tree from thoracic ct scans using a multi-threshold approach. In: Proc. of Second International Workshop on Pulmonary Image Analysis. pp. 341–349. Citeseer (2009)
20. Wang, C., Hayashi, Y., Oda, M., Itoh, H., Kitasaka, T., Frangi, A.F., Mori, K.: Tubular structure segmentation using spatial fully connected network with radial distance loss for 3d medical images. In: International Conference on Medical Image Computing and Computer-Assisted Intervention. pp. 348–356. Springer (2019)
21. Xu, Z., Bagci, U., Foster, B., Mansoor, A., Udupa, J.K., Mollura, D.J.: A hybrid method for airway segmentation and automated measurement of bronchial wall thickness on CT. Medical Image Analysis **24**(1), 1 – 17 (2015)
22. Yun, J., Park, J., Yu, D., Yi, J., Lee, M., Park, H.J., Lee, J.G., Seo, J.B., Kim, N.: Improvement of fully automated airway segmentation on volumetric computed tomographic images using a 2.5 dimensional convolutional neural net. Medical image analysis **51**, 13–20 (2019)
23. Zheng, H., Qin, Y., Gu, Y., Xie, F., Sun, J., Yang, J., Yang, G.Z.: Refined local-imbalance-based weight for airway segmentation in ct. In: International Conference on Medical Image Computing and Computer-Assisted Intervention. pp. 410–419. Springer (2021)
24. Zheng, H., Qin, Y., Gu, Y., Xie, F., Yang, J., Sun, J., Yang, G.Z.: Alleviating class-wise gradient imbalance for pulmonary airway segmentation. IEEE Transactions on Medical Imaging **40**(9), 2452–2462 (2021)
25. Zhou, Z., Rahman Siddiquee, M.M., Tajbakhsh, N., Liang, J.: Unet++: A nested u-net architecture for medical image segmentation. In: Deep learning in medical image analysis and multimodal learning for clinical decision support, pp. 3–11. Springer (2018)